The regulating effects and mechanism of biochar and maifanite on copper and cadmium in a polluted soil-*Lolium perenne* L. system

Yuan DING 1[*], Weiya WANG [1], Shiying AO [1]

[1] *College of Environmental and Chemical Engineering, Nanchang Hangkong University, Nanchang 330063, China*

Corresponding Author:

Yuan DING

No. 696, Fenghe South Avenue, Nanchang, 330063, P. R. CHINA

Email address: 39011@nchu.edu.cn

ABSTRACT

Arable land polluted by copper (Cu) and cadmium (Cd) is a widespread problem. The use of biochar and/or clay mineral as a soil amendment can effectively solidify heavy metals in the soil. We applied biochar (BC), iron modified biochar (Fe-BC), maifanite (MF, a kind of clay minerals), a combination of BC with MF (BC:MF), and Fe-BC with MF (Fe-BC:MF) at a 2 wt % dose as soil amendments to study their ability to prevent Cu and Cd from accumulating in ryegrass (*Lolium perenne L.*). We found that after 90 days of cultivation, the Cd and Cu content both significantly decreased in ryegrass shoots from 2.06 and 209.3 mg kg^{-1}(control) to 1.44 - 2.01 and 51.50 - 70.92 mg kg^{-1}, respectively, across treatments (p< 0.05). Similarly, the bioconcentration factor (BCF) for Cd/Cu was significantly smaller (P< 0.05) in all amendments versus control soil. This trend differed among the shoot, BCF, and transportation factor (TF).

26 Combining BC:MF or Fe-BC:MF did not significantly improve the Cd/Cu stabilization in the
27 soil compared to the corresponding single amendment (p> 0.05). Our adsorption balance
28 experiment showed that BC, Fe-BC, and MF physically and chemically adsorbed Cd and Cu by
29 complexation with functional groups (mesoporous nanomaterials) whose porosity measurements
30 ranged from 0.68 to 78.57 m^2 g^{-1}. Furthermore, the amorphous crystalline iron oxide binding Cd
31 and Cu was the key to immobilizing these metals in the soil. The amendments applied in our
32 study show promise for enhancing immobilization of Cu and Cd in contaminated paddy soils.

33

INTRODUCTION

35 Soil pollution from heavy metals and metalloids is a worldwide concern that affects food
36 production and human health. Anthropogenic activities, such as mining, smelting, military
37 operations, electronic industries, fossil fuel consumption, waste disposal, agrochemical use, and
38 irrigation are the key factors contributing to the increase of heavy metal contents in the soil
39 (Barsova *et al.*, 2019; Liu *et al.*, 2018). Survey data has shown that approximately 19.4% of the
40 total arable land in China has been polluted by various contaminants, among which Cd is highest
41 (Li *et al.*, 2019). The soil in southern China has been seriously contaminated with Cu and Cd
42 near Cu smelters, resulting in large stretches of barren land. It is critical to remediate the polluted
43 soil, restore the natural ecosystem, and protect human health.

44 In-situ chemical immobilization, also known as in-situ solidification/stabilization, is
45 considered to be an inexpensive remediation method to immobilize heavy metals. This method
46 uses chemical reagents, natural minerals, and environmentally friendly waste to decrease heavy
47 metal mobility and phytoavailability. Although the method does not reduce the total amount of
48 heavy metals in the soil, it does minimize the potential transportation of heavy metals from soil
49 to plants (Song *et al.*, 2017). The use of chemical immobilization is still an effective strategy to
50 remediate large areas of contaminated farmland (Shen *et al.*, 2019).

51 Inorganic and organic materials were used extensively in the in situ chemical
52 immobilization of heavy metals. Clay mineral materials, such as sepiolite, smectite, zeolite, and
53 bentonite, are the most effective inorganic amendments to adsorb heavy metals in soil. These can
54 significantly reduce the phytoavailability of heavy metals due to their unique coordination and
55 Si-O tetrahedron and Al-O octahedron structures' adsorption ability (Khalid *et al.*, 2017; Sun *et
56 al.*, 2016). Clay minerals are advantageous in the remediation of heavy metals in soil for their
57 low dosage and high effectiveness. However, there are risks when changing the soil's physical
58 and chemical properties. Recent research has shown that organic amendments prepared from

59   low-cost waste materials decreased the mobility or phytoavailability of heavy metals and
60   improved the soil fertility (Li, Zhou, Qin, Tian, Qi, Yan & Han, 2019; Quan *et al.*, 2020). For
61   example, biochar produced from waste biomass is a typical amendment due to their higher cation
62   exchange capacities (CEC), chemical functional groups, microporous structure, and high pH
63   (Zhai *et al.*, 2018). In acidic soils, the ability to immobilize Cd and Cu was related to soil pH and
64   the number of oxygen-containing groups on the surface of the biochar. Biochar materials were
65   further modified in a variety of ways, such as loading iron hydroxyl group to enhance the surface
66   adsorption capacity (Wan *et al.*, 2020; Zhou *et al.*, 2018).

67   It appears that combining clay minerals with organic amendments, such as biochar, is more
68   suitable for treating contaminated soils. However, the immobile capacity of heavy metals varies
69   greatly with different combinations and applications of organic and inorganic amendments. For
70   instance, Zhang & Ding (2019) investigated the use of hydroxyapatite, bentonite, and biochar,
71   alone or in combination, for remediating Cd-Pb-contaminated soil. Their results showed that the
72   largest reduction in the soluble fraction of Cd and Pb acids was observed under combined
73   amendments. Cu and Cd's phytoavailability and transfer mechanisms in polluted soil still need to
74   be studied with different types, and combinations of, clay minerals and biochar.

75   The accumulation of heavy metals in plants, especially in the shoots, was a direct indicator
76   of the phytoavailability of heavy metals in the soil. However, there were significant differences
77   in amounts due to variations in plant types, as well as the effect of operability. The extraction
78   concentration by a chemical reagent was used to indicate the phytoavailability of heavy metals. It
79   is generally believed that the phytoavailability of Cu and Cd decreases when the weak acid
80   soluble fraction oxidizable and transferred to residual fractions. Soil colloids are an important
81   carrier that can render heavy metals immobile in polluted soils (Tang *et al.*, 2020). Cu and Cd
82   content and fractions in colloids are the key to explaining the immobilization effect and
83   mechanism. Little attention has been paid to the influence of soil colloids on the redistribution
84   and phytoavailability of Cu and Cd in polluted soil. We sought to (1) compare the remediation
85   effects of different types and combinations of biochar and maifanite (a natural clay mineral); (2)
86   understand these amendments' adsorption ability; and (3) elucidate how soil colloids remediate
87   Cu and Cd in polluted soil.

88   **Materials & Methods**

89   **Soil**

90   The soil samples were collected from the plough layer (0-20 cm deep) of a paddy field near
91   a smelter in Jiangxi Province, China (117°12′34″ E and 28°19′6″ N). The soil was air dried at room
92   temperature and passed through a 10 mm sieve to remove stones and roots. The soil's basic
93   physical and chemical properties were: pH: 4.96, soil organic matter (SOM): 2.0 %, cation
94   exchange capacity (CEC): 68.3 mmol kg^{-1}, Cu concentration: 240.0 mg kg^{-1}, Cd concentration:
95   1.93 mg kg^{-1}, Fe concentration: 17.20 mg kg^{-1}, available phosphorous (AP): 5.82 mg kg^{-1}, and
96   available nitrogen (AN): 141.4 mg kg^{-1}.

Biochar testing

98   Biochar was produced from *Radix isatidis* (a component in traditional Chinese medicine)
99   residue. *R. isatidis* was purchased from a pharmacy. The specific preparation method was as
100 follows: deionized (DI) water at a ratio of 500 mL, to which 50 g *radix Isatidis* was added and
101 boiled for approximately 30 min. The dregs were removed and placed in an oven at 105 ℃ for 24
102 h. They were then dried and ground into powder in an agate bowl for later use. A laboratory-
103 scale gas flow-controlled tube-type furnace was used to pyrolyze the *R. isatidis* dreg powder at
104 500 ℃ for 4 h under N$_2$ at a flow rate of 1000 mL min^{-1} to produce biochar. Biochar was further
105 pulverized to 0.25 mm (60 mesh) and marked as BC. The basic properties of final biochar are
106 presented in Table 1.

Modified biochar and maifanite

108 We soaked 20 grams of BC in 1 mol L^{-1} FeCl$_3$ solution, stirred for 10 min, let it sit for 24 h,
109 then filtered and dried it in an 80 ℃ oven. The dried BC was put into muffle furnace for 1 h at
110 500 ℃. After washing, drying, and passing through 60 mesh sieves (0.25 mm), the iron-modified
111 BC was produced and named Fe-BC. The basic properties of Fe-BC are shown in Table 1.

112 Maifanite, a natural SiO$_2$ and NaAlSi$_3$O$_8$ rich mineral, was obtained from a water
113 purification factory using a mesh size of 60-80 (0.18 - 0.25 mm) and named MF (Table 1).

Pot experiment

115 Six treatments were carried out in triplicate for the pot experiment as below: (1) CK,
116 polluted soil as control, (2) BC, Fe-BC, MF, biochar and maifanite BC: MF (1:1, *w/w*), iron
117 modified biochar and maifanite Fe-BC: MF (1:1, *w/w*).

118 A sample of CK (2.00 kg) was completely mixed with amendments (20 g kg^{-1} soil) and

119   transferred to a plastic pot (height: 15 cm; diameter: 17 cm) with deionized (DI) water in a
120   greenhouse at 25 °C. Water content was maintained at 65% of the water holding capacity. No
121   fertilizer was applied to any treatments during the incubation period. Forty ryegrass (*Lolium*
122   *perenne* L.) seeds were spread in each pot 40 days after cultivation. After germination, 20
123   seedlings remained in each pot. The shoots were cut off after 90 days. Soil colloid was extracted
124   from the soil to analyze the fraction distribution of heavy metals after the pot experiment.

Morphology and fraction distribution of amendments before and after

adsorbing Cu and Cd

127   BC, Fe-BC and MF amendments measuring 0.1 g each were passed through a 100-mesh
128   sieve placed in a 50 mL stoppered conical flask. Then, 20 mL standardized solutions of 50 mg L^{-1}
129   Cu and Cd were added to the flask. We added a 0.01 mol L^{-1} NaCl solution to simulate soil
130   conditions, followed by the addition of 0.01 mol L^{-1} HCl and 0.01 mol L^{-1} NaOH solutions to
131   adjust the pH value to 4.96, which was the pH value of the soil. Samples were kept at a constant
132   room temperature for 24 h before centrifugation and filtration. The amendments were dried in an
133   oven at 60 °C after the adsorption of Cu and Cd and crushed in an agate bowl to a particle size of
134   100 mesh for heavy metal morphology and fraction distribution analysis.

Cu and Cd content in ryegrass (*L. perenne* L.)

136   The air-dried ryegrass samples were ground into powder using a pulverizer to detect the
137   heavy metal content. Next Cu and Cd content were measured using microwave digestion
138   combined with flame-graphite furnace atomic absorption spectrometry. Cu and Cd were then
139   measured using the FAAS/GFAAS method (GB/T 17138-1997 and GB/T 17141-1997).

Fraction analysis of heavy metals in soil and soil colloid

141   Soil heavy metal fraction analysis can be divided into a weak acid soluble fraction, a
142   reducible fraction, an oxidizable fraction, and a residue fraction according to the BCR sequential
143   extraction method. The modified BCR sequential extraction procedures were used for heavy
144   metal fraction analysis in the soil (Zhang *et al.*, 2019). Heavy metal fractions in soil colloid can
145   be classified as an amorphous iron oxide bound fraction, a crystalline iron oxide bound fraction,
146   and a residue fraction (Yin *et al.*, 2016).

147 **Amendment microcharacters before and after adsorption**

148   Modified BCR sequential extraction procedures were used for heavy metal fraction analysis
149 in the amendments (Zhang, Shao, Zhang, Zhang & Chen, 2019).

150   Amendments' specific surface area (SSA) values were measured using a Tristar II type
151 3020 (V1.04) analyzer (Micromeritics Instrument, USA). A scanning electron microscope (SEM,
152 SU1510, Hitachi, Japan) was used to observe the surface morphology and microstructure. The
153 samples were mounted on a carbon stub and were coated with Au before the examination. The
154 crystal structures of the amendments were examined using the x-ray diffraction analysis
155 technique (XRD, D8 Advance X-ray diffractometer, Bruker) before and after adsorption. The
156 surface functional groups of biochar and maifanite were determined using the Fourier transform
157 infrared spectroscopy technique (FTIR, Vertex 70, Bruker, Germany).

158 **Calculation and statistical analysis**

159   The bioconcentration factor (BCF) and the transportation factor (TF) were calculated using the
160 following equations (Zhang et al., 2020):

161 $$BCF = \frac{C_{shoot} + C_{root}}{C_{soil}}$$

(1)

162 $$TF = \frac{C_{shoot}}{C_{root}}$$

(2)

163 Where C_{shoot} is the metal concentration in the ryegrass shoots (mg kg^{-1}), C_{root} is the metal
164 concentration in the root of ryegrass (mg kg^{-1}), and C_{soil} is the metal concentration in the soil
165 (mg kg^{-1}).

166   The data were subjected to one-way analysis of variance (ANOVA) using SPSS software
167 (version 23.0). Duncan's multiple range test was performed to determine the difference between
168 treatments. Means were compared using the least significant difference test at a $p < 0.05$ level of
169 significance, and letters were used to suggest the significant variations in the data set. All of the
170 results in the tables and figures were described as means ± standard deviation (n = 3).

171   The precision and accuracy of heavy metal analysis were assessed through repeated analysis

172   of the samples against National Institute of Standard and Technology, Standard Reference

173   Material (GBW07408, National Standard Detection Research Center, Beijing, China) for all the

174   heavy metals. The results were found to be within ±2% of the certified value. Variations were

175   found to be less than 10%.

Results and Discussion

Immobilizing different amendments on Cu and Cd in soil

Effect on ryegrass

179   *L. perenne* L. is a good indicator of heavy metal polution in soil as they are resistant to Cu

180   and Cd. Ryegrass can enter the food chain as a kind of pasture, therefore, we analyzed Cu and

181   Cd content change in ryegrass shoots after the addition of different amendments (Fig. 1).

182   As shown in Fig. 1A, Cu content in shoots significantly decreased from 209.3 mg kg^{-1} (CK)

183   to 51.50 mg kg^{-1} (BC), 57.90 mg kg^{-1} (Fe-BC:MF), 59.29 mg kg^{-1} (BC:MF), 63.74mg kg^{-1} (MF),

184   and 70.92 mg kg^{-1} (Fe-BC). Cd also decreased from 2.06 mg kg^{-1} (CK) to 1.43 mg kg^{-1} (MF),

185   1.46 mg kg^{-1} (BC), 1.51 mg kg^{-1} (BC:MF), 1.53 mg kg^{-1} (Fe-BC), and 2.01 mg kg^{-1} (Fe-BC:MF).

186   Cu was immobilized in the following order: BC > Fe-BC:MF ≈ BC:MF > MF ≈ Fe-BC. Cu

187   content decreased by 75.4%, 72.3%, 71.7%, 69.6%, and 66.1%, respectively, compared with the

188   control. By contrast, Cd immobilized in shoots after treatment with Fe-BC:MF did not differ

189   significantly from the control ($P > 0.05$). The treatments BC, Fe-BC, MF, and BC:MF

190   significantly reduced the Cd content in ryegrass shoots by 29.3%, 25.8%, 30.4%, and 26.9 %,

191   respectively.

192   The absorption of Cu and Cd in ryegrass shoot revealed the significant resistance effects of

193   the amendments except for Fe-BC:MF. Furthermore, the resistance effect on Cu was much

194   greater than on Cd according to the decreasing amplitude of the heavy metal content in the shoot.

195   Our results was confirmed by Xu & Zhao (2013), who adopted biochar to adsorb Cu(II), Cd(II)

196   and Pb(II) in soil from southern China, and found that the complexing ability of the biochars

197   with Cu(II) and Pb(II) was much stronger than that with Cd(II) and induced more specific

198   adsorption of Cu(II) and Pb(II) by the soils than that of Cd(II).

199   The combination amendment of Fe-BC and MF or BC and MF did not show better

200   advantage than the corresponding sole amendment ($p > 0.05$).

Effect of different amendments on BCF of Cu and Cd

202   BCF reflects the capacity of the plant as a whole (including shoot and root) to uptake Cu
203   and Cd from the soil. This indicator is significant in plants that enter the food chain because it
204   fully expresses the total amount of heavy metals taken up from the soil.

205   The BCF value for Cu and Cd was significantly ($p < 0.05$) smaller in any amendment than
206   that in the unamended soil (Figure 2). However, the trend and reducing amplitude of the BCF
207   value were not consistent with the corresponding heavy metal content in the ryegrass shoot. The
208   BCF value for Cu decreased from 4.82 (CK) to 2.75-3.89 (amendments). The value decreased for
209   Cd from 4.92 (CK) to 2.55-3.54 after the application of amendments. In addition, the best
210   immobilization effect of the BCF value on Cu is MF, and Fe-BC of Cd, among the amendments.

Different amendments' effects on TF of Cu and Cd

212   The content of Cu and Cd in ryegrass shoots was inconsistent with the corresponding value
213   of BCF. This effect may be due to the varying transfer capacity of Cu and Cd from root to shoot
214   after being treated with different amendments. The changes in Cu and Cd with the transportation
215   factor (TF) are shown in Fig 3.

216   TF is an important indicator of the transportation of heavy metals in plant tissues (Zhang et
217   al., 2020). Fig. 3A shows that the TF value of Cu (0.07-0.11) was significantly smaller than that
218   of the control group (0.22), indicating that the transfer ability of Cu from the root to the shoot
219   also decreased after the application of the amendment. However, the TF value of Cd (0.28 - 0.50)
220   was significantly larger than that of the control group (0.28) (Fig. 3B).

221   As an essential element, copper is beneficial to the environment in trace quantities and be
222   poisonous at high concentration. However, the total Cu content in the soil (239.98 mg kg^{-1}) in
223   our study was so high that ryegrass exerted a self-protection mechanism to prevent Cu transfer
224   from root to shoot, even after amendments were applied to decrease its phytoavailability (Ali *et*
225   *al.*, 2017). Therefore, the value of BCF and TF of copper was still less than the control after the
226   application of amendments.

227   Cadmium is a non-essential element for plant growth and shows carcinogenicity. A high
228   content of Cd would inhibit plant growth or even cause death, but low content would promote
229   plant growth. Low amounts of Cd in the soil will also promote Cd transport from root to shoot.
230   Limited Cd content (0.30 mg kg^{-1}) in China's soil environmental quality standard (GB 15618-
231   2018) is within the range required to promote plant growth and absorption. Research has shown
232   that Cd content in test plant such as rice and peanuts is higher than food hygiene standards, while
233   the soil Cd content is lower than the soil standard (Gallego *et al.*, 2012). In the same way, the

234   bioavailable Cd content after immobilization may be within a range that is easily transferred and
235   absorbed by plants. This may be the reason that the TF of cadmium treated with the amendments
236   increased in our study.

Microscopic characteristics of amendments and its interaction mechanism with Cu and Cd

Micromorphology and specific surface area of amendments

240   As described above, the sole amendment by BC, Fe-BC, MF and their combinations clearly
241   immobilized Cd and Cu in polluted soil. We determined the amendments' micromorphology and
242   the fraction distribution of Cd and Cu in the amendments and soil colloid. This illuminates the
243   microcharacteristic differences of these amendments (BC, Fe-BC, MF) and its immobilization of
244   Cd and Cu.

245   The three amendments' morphologies were examined with SEM. The BC amendment
246   showed an irregular microstructure with an uneven surface and dense distribution of pore
247   channels (Fig. 4A). Tiny particles attached to Fe-BC's surface may be iron oxides (Fig. 4B),
248   which was consistent with the data in Table 1. The content of iron increased from 4.66 g kg^{-1} to
249   172.9 g kg^{-1} after being modified by iron salt. The iron oxides on the surface of the biochar may
250   be Fe_3O_4 or α-FeOOH, which provide abundant active hydroxyl groups for biochar (Zhu *et al.*,
251   2019). The MF amendment (Fig. 3C) revealed a distinct layered structure and a large number of
252   granular particles attached to its surface.

253   In addition to SEM, BET was also used to determine the specific surface area (SSA) of the
254   materials. The results showed that all of the studied amendments belonged to mesoporous
255   nanomaterials with SSA values at the range of 0.68-78.57 m^2 g^{-1} (Table 1). The highest SSA
256   value was detected in Fe-BC, indicating that Fe-BC could provide more adsorption of Cu and Cd
257   than others.

Functional groups of amendments before and after adsorption of Cu and Cd

260   We analyzed the variations of the functional groups of the amendments before and after Cu
261   and Cd adsorption using the FTIR spectroscopy technique (Fig. 5). The wide absorption peaks at

262   1,110 cm^{-1} were characteristic of the thermal degradation of lignocellulosic biomass, mainly
263   generated by the vibrations caused by the expansion of C-O bonds (Wu *et al.*, 2018). There was
264   almost no change noted in the characteristic peaks of Fe modified/unmodified biochar after the
265   adsorption of heavy metals (Fig. 5A), indicating that there was limited damage made to the
266   lignocellulosic structure.

267   The surface functional groups of BC detected at 1,700 cm^{-1}, 1,560 cm^{-1}, and 1,380 cm^{-1}
268   were assigned to the carbonyl (C=O) (Wang *et al.*, 2014). The C=C bending vibration, CH$_3$
269   bending vibrations (Hao *et al.*, 2021), and the hydroxyl (-OH) appeared at 1,420 cm^{-1} and 617
270   cm^{-1}(Bueno & Morgado, 1993; Mitić *et al.*, 2009). The results demonstrated that the surface of
271   the biochar from medicine residue included oxygen-containing functional groups, such as
272   carboxyl, lactone, carbonyl, and hydroxyl. The strength of the framework-stretching vibration
273   absorption peak of C=O in the aromatic ring at 1,700 cm^{-1} decreased after the adsorption of Cu
274   and Cd. The characteristic peak for the -OH functional group of BC decreased at 1,420 cm^{-1},
275   indicating that the hydroxyl groups possibly on the surface of the biochar may participate in the
276   adsorption reaction process of Cu and Cd. Consequently, the BC surface, a type of porous
277   material with the oxygen-containing functional groups mentioned above, was involved in the
278   adsorption reaction process of Cu and Cd.

279   The absorption peak of CH$_3$ bending vibrations at 1,380 cm^{-1} for Fe-BC was stronger than
280   BC when comparing BC with Fe-BC before adsorption. The C=O absorption peak (1,700 cm^{-1}),
281   and -OH bending vibration peak (1,420 cm^{-1} and 617 cm^{-1}) for Fe-BC practically disappeared.
282   The absorption peak of Fe-OH at 796 cm^{-1} appeared (Chen *et al.*, 2020), which is a characteristic
283   peak for iron oxide, signaling that Fe was attaching on the surface of the biochar. The absorption
284   peak at 796 cm^{-1} and 1,380 cm^{-1} significantly weakened after the adsorption of heavy metals with
285   Fe-BC, implying that Fe-OH and -CH$_3$ participated in the reaction process.

286   In addition, the FTIR spectra of Fe-BC samples (Fig. 5A) and maifanite samples after
287   adsorption of Cu and Cd (Fig. 5B) showed a vibration peak of –OH group related to water at
288   3,380 cm^{-1} or 3,450 cm^{-1}. Moisture was unavoidable in the experiments.

289   MF is rich in quartz, feldspar, and smectite, as aforementioned. The stretching vibrational
290   peak corresponding to C=O and can be detected at a wavenumber of 1,800 cm^{-1}, and the bending
291   vibration peak of H-O-H at 1,630 cm^{-1}. The stretching vibration absorption peak of Si-OH was
292   detected at 1,030 cm^{-1}. The FTIR absorption peaks intensies weakened after Cu and Cd
293   adsorption, indicating the main components participated in the adsorption of heavy metals
294   (Zhang *et al.*, 2012).

X-ray diffraction analysis of amendments before and after adsorption

295

296 Carbon was a main component in the biochar produced from the medicine residue of *radix*
297 *Isatidis*. Patterns of XRD in Fig. 6A reveal a wide and slow diffusion peak in the range of 22°-36°
298 for C (002), which is typically caused by the lamination of single atomic carbon layers in
299 microcrystals. Moreover, C (101) of cellulose characteristic crystal plane diffraction peaks with
300 relatively wide but small intensity was observed in the range of 12°-15°. We also detected
301 characteristic peaks from SiO_2 at 26.48°, $CaCO_3$ at 29.56° and 43°, and $CaMg(CO_3)_2$ at 30.8°
302 when comparing the resulting patterns with the standard pdf cards. The results showed the
303 presence of SiO_2, $CaCO_3$, and $CaMg(CO_3)_2$ on the biochar surface when the biochar was formed
304 in the process of gasification evaporation. Our results are similar to those of Wang *et al.* (2017),
305 which detected alkaline salts, such as KCl, $CaCO_3$, and $MgCl_2$ in the biochar extracted from
306 water hyacinth and maize straw.

307 There were no clear changes in diffraction peak positions after the adsorption of Cu and
308 Cd in BC were observed. C, SiO_2, $CaCO_3$, and $CaMg(CO_3)_2 SiO_2$ did not participate in Cu and
309 Cd reactions. In addition, Cu^{2+} and Cd^{2+} were adsorbed on the surface of biochar with organic
310 groups, such as hydroxyl, carboxyl, lactone, and carbonyl. We detected characteristic peaks of C,
311 SiO_2, $CaCO_3$, and $CaMg (CO_3)_2 SiO_2$ as well as magnetite in the X-ray diffraction pattern of Fe-
312 BC (Fig. 6A). This observation indicates that the iron oxide loaded to BC might be magnetite.

313 The XRD peaks of maifanite after the adsorption of Cu and Cd (Fig. 6B) reveal the
314 presence of SiO_2, $CaCO_3$, $NaAlSi_3O_8$ (sodium feldspar), and $Al_2Si_2O_5(OH)_4$ (smectite). The
315 absorption peaks of smectite at 10.4° and 12.3° disappeared after adsorption of Cu and Cd. The
316 absorption peaks of sodium feldspar at 8.75°, 13.8°, and 27.3° also weakened or disappeared
317 completely as a result of Cu and Cd adsorption. These results indicate that the silica hydroxyl,
318 hydroxyl, and carboxyl groups on the surface of sodium feldspar and smectite in maifanite
319 participate in the adsorption of Cu and Cd. Analyses of SEM, FTIR, and XRD in the
320 immobilization process are consistent.

321 *Extraction fraction of heavy metals from amendments*

322 BC, Fe-BC, and MF are mesoporous nanomaterials, which physically adsorbed Cu and Cd
323 and generated a chemical complexation with functional groups on their surfaces. This affected
324 the extraction fraction percentage of Cu and Cd across amendments.

325 The modified BCR sequential extraction method was used to analyze the Cu and Cd
326 fraction from the amendments after adsorption (Fig. 7). The weak acid soluble fractions of Cu in

327 MF, BC, and Fe-BC were 91.10%, 41.06%, and 52.65%, respectively. The reducible fractions of
328 Cu were 1.59%, 10.03%, and 9.65%, respectively. The oxidizable fractions of Cu were 0.08%,
329 15.00%, and 11.98%, respectively, and the residual fractions of Cu were 7.23%, 33.92%, and
330 25.72%, respectively, after the adsorption equilibrium experiment. The residual fraction Cu in
331 balanced MF with Cu and Cd solution was significantly lower than that in balanced BC and
332 balanced Fe - BC, which was inconsistent with the results in treated soil. The residual fraction
333 Cu in soil treated with MF was the highest among all of the amend treatments (Fig S1). The pH
334 of the solution in the adsorption balance experiment was affected by the amendments. The pH of
335 MF (7.03) was neutral and lower than that of BC (10.93) and Fe-BC (8.44) (Table 1). The
336 immobile effect of MF on heavy metals was worse than that of BC and Fe-BC. The soil pH was
337 6.30, 5.99 and 5.77, respectively, after being treated with the test amendments. The change of pH
338 in test soils was not consistent with the solution, in which MF increased the soil pH most
339 significantly. Thus the increase in heavy metal residual fraction in the soil was the most
340 significant among the three amendments.

341   The weak acid soluble fractions of Cd in MF, BC, and Fe-BC were 97.24%, 86.14%, and
342 84.38%. The reducible fractions of Cd were 0.48%, 12.09%, and 13.18%. The oxidizable Cd
343 fractions were undetected. The residual fractions of Cd were 2.28%, 1.16% and 1.82%,
344 respectively, after the adsorption equilibrium between amendments and the Cu, Cd solution (Fig.
345 7B). The residual fractions of heavy metals in soil were generally not absorbed by the plants. The
346 residual fraction of Cu in all treatments was far higher than Cd, indicating that the immobile
347 effect of the three amendments on Cu was better than that on Cd. These results are consistent
348 with the content of Cu and Cd in ryegrass after treatment.

Extraction fraction of heavy metals from soil colloid with amendments

350 The heavy metals and the soil colloid interacted with the amendment in the soil environment.
351 Soil colloids are the basic soil functional unit carrying heavy metals due to its small particle size,
352 larger SSA and negative charge. It was also a key factor affecting the distribution of heavy
353 metals in the soil. Therefore, the total content of Cu and Cd in colloids was much higher than
354 that in the soil (Table 2). For example, the content of Cu and Cd in untreated polluted soil
355 colloids was 489.92 mg kg^{-1} and 2.57 mg kg^{-1}, respectively, which was 2.04 and 1.33 times that
356 of soil Cu (239.98 mg kg^{-1}) and Cd (1.93 mg kg^{-1}). The accumulation effect on Cu is greater than
357 Cd in colloid.

358   Heavy metals in soil colloids can be divided into an amorphous iron oxide bound fraction, a
359 crystal iron oxide bound fraction and a residual bound fraction. It is well known that the increase

360 of the amorphous iron oxide bound fraction signals the decrease in the phytoavailability of heavy
361 metals. The forms of Cu and Cd in the soil colloid after treated with MF, BC and Fe-BC were all
362 relocated (Figure 8). Compared with the CK treatment, the content of amorphous/non-crystalline
363 iron oxide-bond Cu in colloids after immobilization treatments increased significantly by 20.34%,
364 16.81%, and 18.87%, respectively. The content of residual bond Cu decreased significantly by
365 20.23%, 17.01%, and 19.17%, respectively. Non-crystalline iron oxide bond Cd content
366 increased significantly by 3.72%, 4.18%, and 6.58%, respectively, and the residual bond Cd
367 decreased significantly by 3.65%, 4.57%, and 7.04%, respectively. The variation in the
368 crystalline iron oxide bond of Cu or Cd was not significant. The effect of amendments on Cu was
369 greater than Cd. Moreover, soil endogenetic minerals and organic matter may participate in the
370 immobilization process, affecting the redistribution of heavy metals in the soil and soil colloid.

Conclusions

371

372 The studied amendments, BC, Fe-BC, MF, BC:MF(1:1), and Fe-BC:MF(1:1), effectively
373 immobilized copper and cadmium, and the types and combinations of BC and MF used affected
374 Cu and Cd differently. Amendments were better able to immobilize Cu than Cd. The Cu content
375 in shoots significantly decreased from 209.3 mg kg^{-1} (CK) to 51.50 mg kg^{-1} (BC), 57.90 mg kg^{-1}
376 (Fe-BC:MF), 59.29 mg kg^{-1} (BC:MF), 63.74mg kg^{-1} (MF), and 70.92 mg kg^{-1} (Fe-BC).
377 Meanwhile, the Cd content decreased from 2.06 mg kg^{-1} (CK) to 1.43 mg kg^{-1} (MF), 1.46 mg kg^{-1}
378 (BC), 1.51 mg kg^{-1} (BC:MF), 1.53 mg kg^{-1} (Fe-BC), and 2.01 mg kg^{-1} (Fe-BC:MF).

379 BC, Fe-BC, and MF may physically adsorb copper and cadmium. They may also generate
380 chemical complexation with functional groups which could then affect the extraction fraction
381 percentage of Cu and Cd in the amendments. The content of amorphous crystalline iron oxide
382 bound Cu in colloid was higher than Cd, and was a key step to immobilization.

383 The studied amendments can be used to enhance the immobilization of copper and
384 cadmium in the contaminated paddy soils. The immobilization effects of the amendments
385 depended on the metal element and combination of amendments. The suitable amendment
386 method outlined in this research may be used to prevent the contamination of heavy metals in
387 soils, especially Cu and Cd.

References

388

389 Ali A, Guo D, Zhang Y, Sun X, Jiang S, Guo Z, Huang H, Liang W, Li R, and Zhang Z.

390   2017. Using bamboo biochar with compost for the stabilization and phytotoxicity reduction of

391   heavy metals in mine-contaminated soils of China. *Scientific Reports* 7:2690.

392   Barsova N, Yakimenko O, Tolpeshta I, and Motuzova G. 2019. Current state and dynamics

393   of heavy metal soil pollution in Russian Federation-A review. *Environmental Pollution* 249:200-

394   207.

395   Bueno WA, and Morgado F. 1993. Hydrogen bonding of adenine with benzoic acids in the

396   solid state. An FTIR study. *Spectrochimica Acta Part A: Molecular Spectroscopy* 49:249-256.

397   Chen M, Lu G, Wu J, Sun J, Yang C, Xie Y, Wang K, Deng F, Yi X, and Dang Z. 2020.

398   Acidity and metallic elements release from AMD-affected river sediments: Effect of AMD

399   standstill and dilution. *Environmental Research* 186:109490.

400   Gallego SM, Pena LB, Barcia RA, Azpilicueta CE, Iannone MF, Rosales EP, Zawoznik MS,

401   Groppa MD, and Benavides MP. 2012. Unravelling cadmium toxicity and tolerance in plants:

402   Insight into regulatory mechanisms. *Environmental & Experimental Botany* 83:33-46.

403   Hao N, Cao J, Ye J, Zhang C, Li C, and Bate B. 2021. Content and morphology of lead

404   remediated by activated carbon and biochar: A spectral induced polarization study. *Journal of*

405   *Hazardous Materials* 411:124605.

406   Khalid S, Shahid M, Niazi NK, Murtaza B, Bibi I, and Dumat C. 2017. A comparison of

407   technologies for remediation of heavy metal contaminated soils. *Journal Of Geochemical*

408   *Exploration* 182:247-268.

409   Li CF, Zhou KH, Qin WQ, Tian CJ, Qi M, Yan XM, and Han WB. 2019. A Review on

410   Heavy Metals Contamination in Soil: Effects, Sources, and Remediation Techniques. *Soil &*

411   *Sediment Contamination* 28:380-394.

412   Liu LW, Li W, Song WP, and Guo MX. 2018. Remediation techniques for heavy metal-

413   contaminated soils: Principles and applicability. *Science Of the Total Environment* 633:206-219.

414   Mitić Ž, Nikolić GS, Cakić M, Premović P, and Ilić L. 2009. FTIR spectroscopic

415   characterization of Cu(II) coordination compounds with exopolysaccharide pullulan and its

416   derivatives. *Journal of Molecular Structure* 924-926:264-273.

417   Quan G, Fan Q, Sun J, Cui L, Wang H, Gao B, and Yan J. 2020. Characteristics of organo-

418   mineral complexes in contaminated soils with long-term biochar application. *Journal of*

419   *Hazardous Materials* 384:121265.

420   Shen Z, Jin F, O'Connor D, and Hou D. 2019. Solidification/stabilization for soil

421   remediation: An old technology with new vitality. *Environmental Science & Technology*

422   53:11615-11617.

423   Song B, Zeng GM, Gong JL, Liang J, Xu P, Liu ZF, Zhang Y, Zhang C, Cheng M, Liu Y,

424   Ye SJ, Yi H, and Ren XY. 2017. Evaluation methods for assessing effectiveness of in situ

425   remediation of soil and sediment contaminated with organic pollutants and heavy metals.

426   *Environment International* 105:43-55.

427   Sun YB, Sun GH, Xu YM, Liu WT, Liang XF, and Wang L. 2016. Evaluation of the

428 effectiveness of sepiolite, bentonite, and phosphate amendments on the stabilization remediation

429 of cadmium-contaminated soils. *Journal Of Environmental Management* 166:204-210.

430 Tang XY, Katou H, and Suzuki K. 2020. Liming effects on dissolved and colloid-associated

431 transport of cadmium in soil under intermittent simulated rainfall. *Journal of Hazardous*

432 *Materials* 400:123244.

433 Wan X, Li C, and Parikh SJ. 2020. Simultaneous removal of arsenic, cadmium, and lead

434 from soil by iron-modified magnetic biochar. *Environmental Pollution* 261:114-157.

435 Wang H, Xia W, Lu P, Bu Y, and Yang H. 2017. Adsorption characteristics of biochar on

436 heavy metals (Pb and Zn) in soil. *Environmental Science* 38:3944-3952.

437 Wang S, Lin H, Ru B, Sun W, Wang Y, and Luo Z. 2014. Comparison of the pyrolysis

438 behavior of pyrolytic lignin and milled wood lignin by using TG–FTIR analysis. *Journal of*

439 *Analytical and Applied Pyrolysis* 108:78-85.

440 Wu X, Ba Y, Wang X, Niu M, and Fang K. 2018. Evolved gas analysis and slow pyrolysis

441 mechanism of bamboo by thermogravimetric analysis, Fourier transform infrared spectroscopy

442 and gas chromatography-mass spectrometry. *Bioresource Technology* 266:407-412.

443 Xu R, and Zhao A. 2013. Effect of biochars on adsorption of Cu(II), Pb(II) and Cd(II) by

444 three variable charge soils from southern China. *Environmental Science and Pollution Research*

445 20:8491-8501.

446   Yin H, Tan N, Liu C, Wang J, Liang X, Qu M, Feng X, Qiu G, Tan W, and Liu F. 2016. The

447   associations of heavy metals with crystalline iron oxides in the polluted soils around the mining

448   areas in Guangdong Province, China. *Chemosphere* 161:181-189.

449   Zhai X, Li Z, Huang B, Luo N, Huang M, Zhang Q, and Zeng G. 2018. Remediation of

450   multiple heavy metal-contaminated soil through the combination of soil washing and in situ

451   immobilization. *Science of the Total Environment* 635:92–99.

452   Zhang D, and Ding A. 2019. Effects of Passivating Agents on the Availability of Cd and Pb

453   and Microbial Community Function in a Contaminated Acidic Soil. *Bulletin of Environmental*

454   *Contamination and Toxicology* 103:98-105.

455   Zhang H, Shao J, Zhang S, Zhang X, and Chen H. 2019. Effect of Phosphorus-Modified

456   Biochars on Immobilization of Cu (II), Cd (II), and As (V) in Paddy Soil. *Journal of Hazardous*

457   *Materials* 390:121349.

458   Zhang L, Luo L, and Zhang S. 2012. Integrated investigations on the adsorption mechanisms

459   of fulvic and humic acids on three clay minerals. *Colloids and Surfaces A* 406:84-90.

460   Zhang S, Gong X, Shen Z, Yuan S, and Wang G. 2020. Study on Remediation of Cd-

461   Contaminated Soil by Thermally Modified Attapulgite Combined with Ryegrass. *Soil and*

462   *Sediment Contamination* 29:1-22.

463   Zhou X, Liu Y, Zhou J, Guo J, Ren J, and Zhou F. 2018. Efficient removal of lead from

464   aqueous solution by urea-functionalized magnetic biochar: Preparation, characterization and

465   mechanism study. *Journal of the Taiwan Institute of Chemical Engineers* 91:457-467.

466   Zhu M, Hu X, Tu C, Zhang H, Song F, Luo Y, and Christie P. 2019. Sorption mechanisms

467   of diphenylarsinic acid on ferrihydrite, goethite and hematite using sequential extraction, FTIR

468   measurement and XAFS spectroscopy. *Science of the Total Environment* 669:991-1000.

469

470

Basic properties of biochar and maifanite

BC: biochar from medicine residue, Fe-BC: iron modified biochar, MF: maifanite. "ND" indicates undetected or below the detection limit. Values were described as means± standard deviation (n=3).

1 **Table 1 Basic properties of biochar and maifanite#**

Treatment	pH	Cu/mg kg^{-1}	Cd/mg kg^{-1}	Fe/g kg^{-1}	ash content/%	SSA/m^2 g^{-1}
BC	10.93±0.09	18.49±0.59	ND	4.66±0.51	13.73±0.62	9.45
Fe-BC	8.44±0.03	26.80±0.94	ND	172.9±5.0	26.24±1.26	78.57
MF	7.03±0.18	12.89±0.53	ND	ND	ND	0.68

2 **Notes.**

3 BC: biochar from medicine residue, Fe-BC: iron modified biochar, MF: maifanite. "ND" indicates undetected or below the

4 detection limit. Values were described as means± standard deviation (n=3).

Effect of amendments on the content of Cu and Cd in soil colloid.

1 **Table 2 Effect of amendments on the content of Cu and Cd in soil colloid.**

treatment	CK	MF	BC	Fe-BC
Cu/mg·kg^{-1}	489.9±8.4a	488.1±11.4a	500.5±24.2a	471.0±8.8a
Cd/mg·kg^{-1}	2.57±0.04b	2.17±0.23a	2.35±0.53a	1.98±0.06a

Figure 1

Cu (A) and Cd (B) content in shoot of ryegrass treated with different amendments.

The data shown here was the averages of three replicates with the standard error indicated by the vertical bars. Different lowercase letters in each column represented statistically significant differences among treatments (P<0.05).
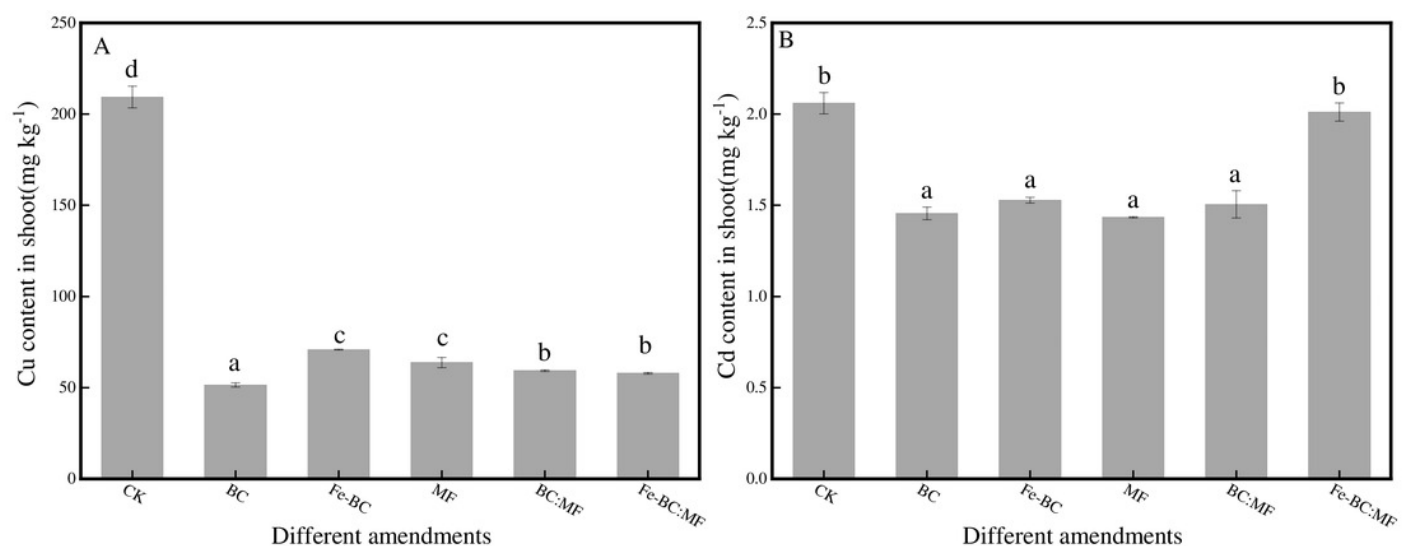
Figure 2

Effects of different amendments on BCF of Cu and Cd (A and B).
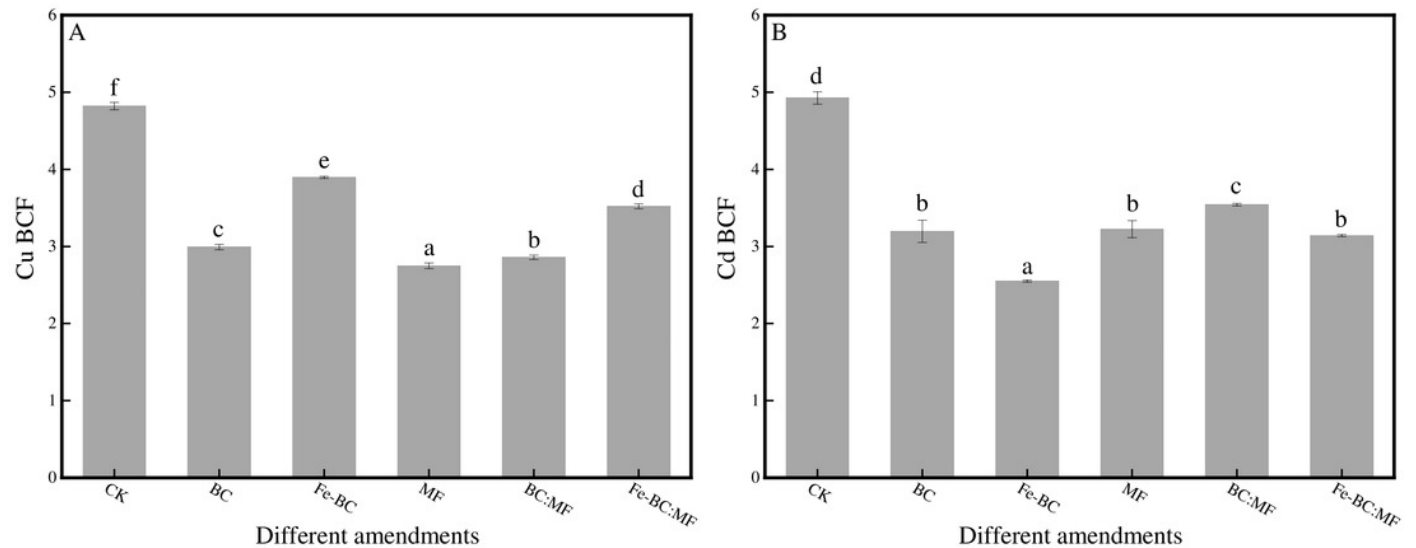
Figure 3

Effects of different amendments on transportation factor for Cu (A) and Cd (B).
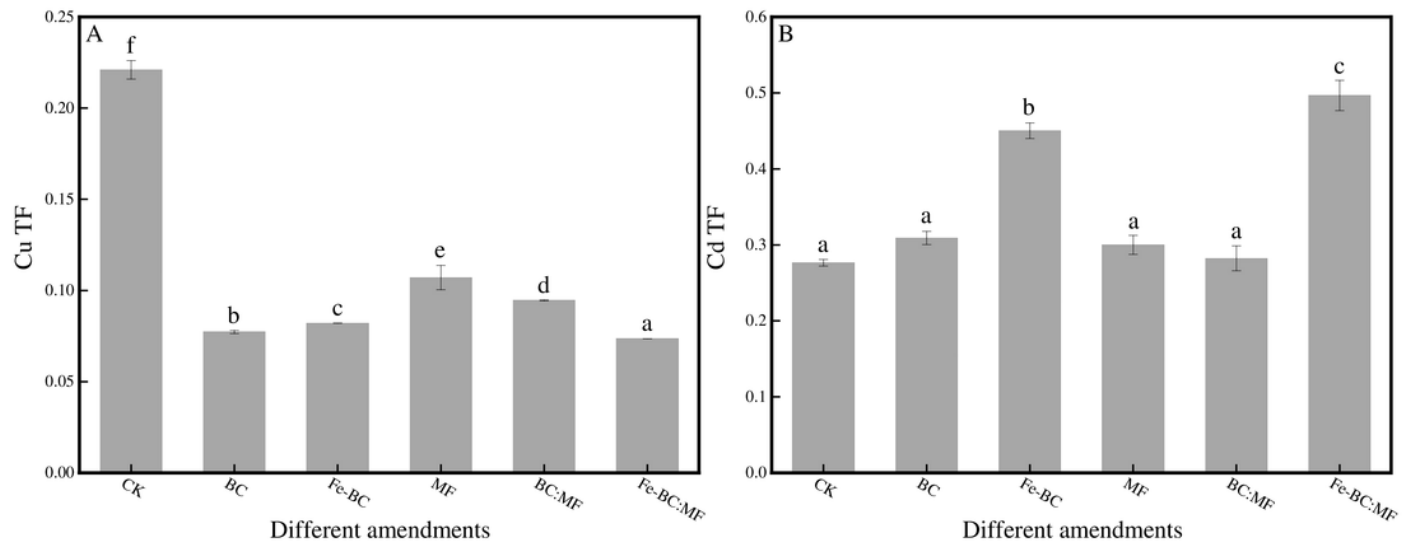
Figure 4

Scanning electron microscopy (SEM) micrographs of amendments BC (A), Fe-BC (B), and MF (C).
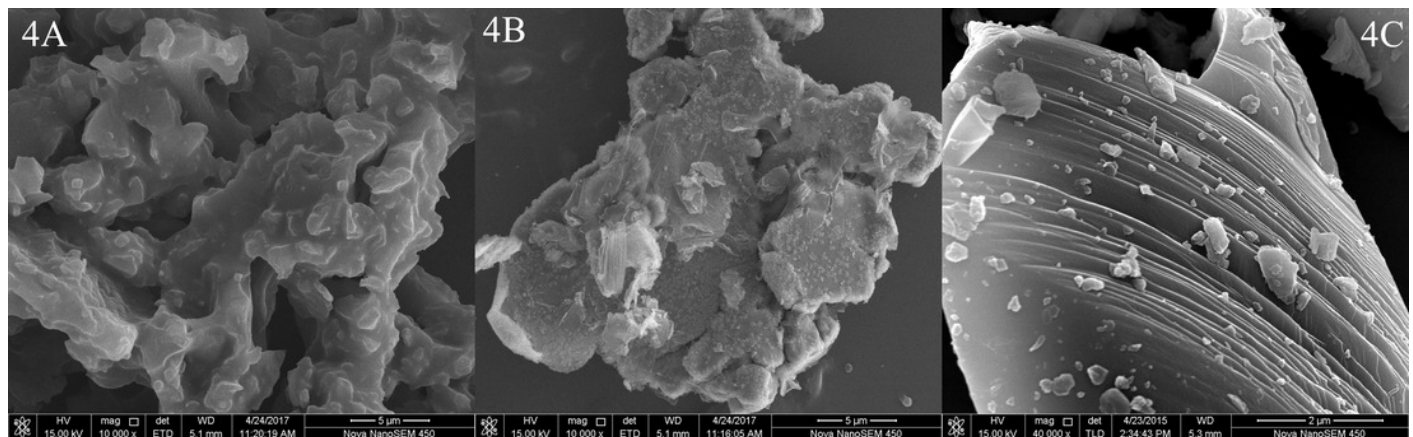
Figure 5

FTIR spectra of BC and Fe-BC500 (A), and MF (B) before and after adsorption of Cu and Cd.
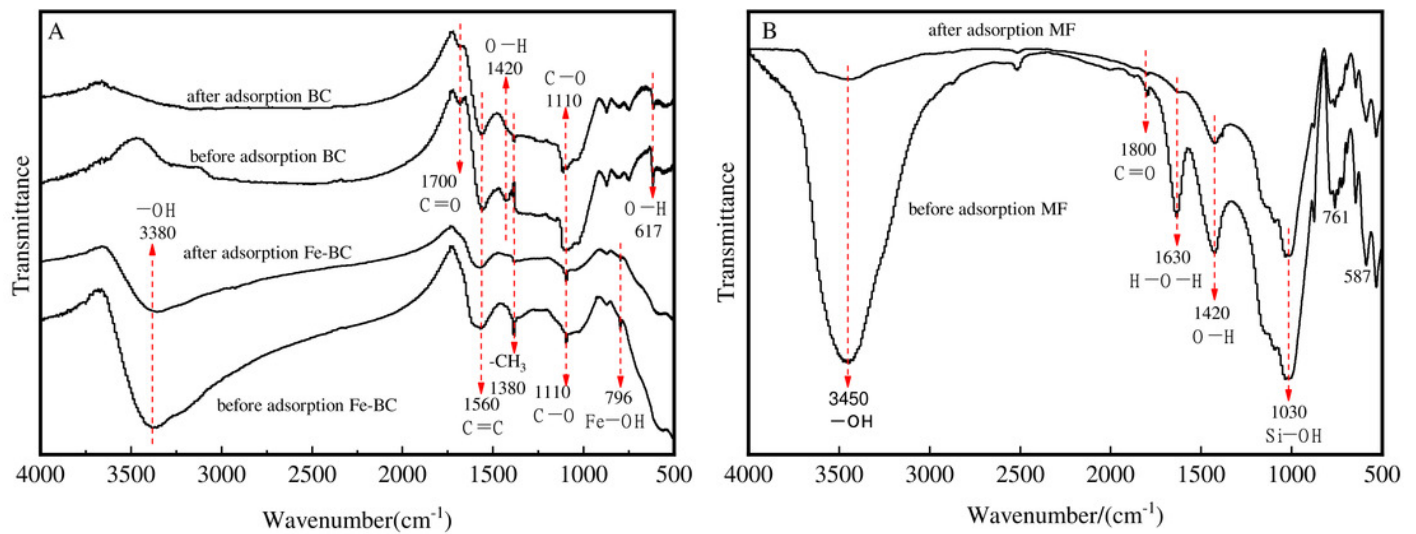
Figure 6

XRD patterns of BC and Fe-BC (A) and MF (B) amendments before and after adsorption of Cu and Cd.
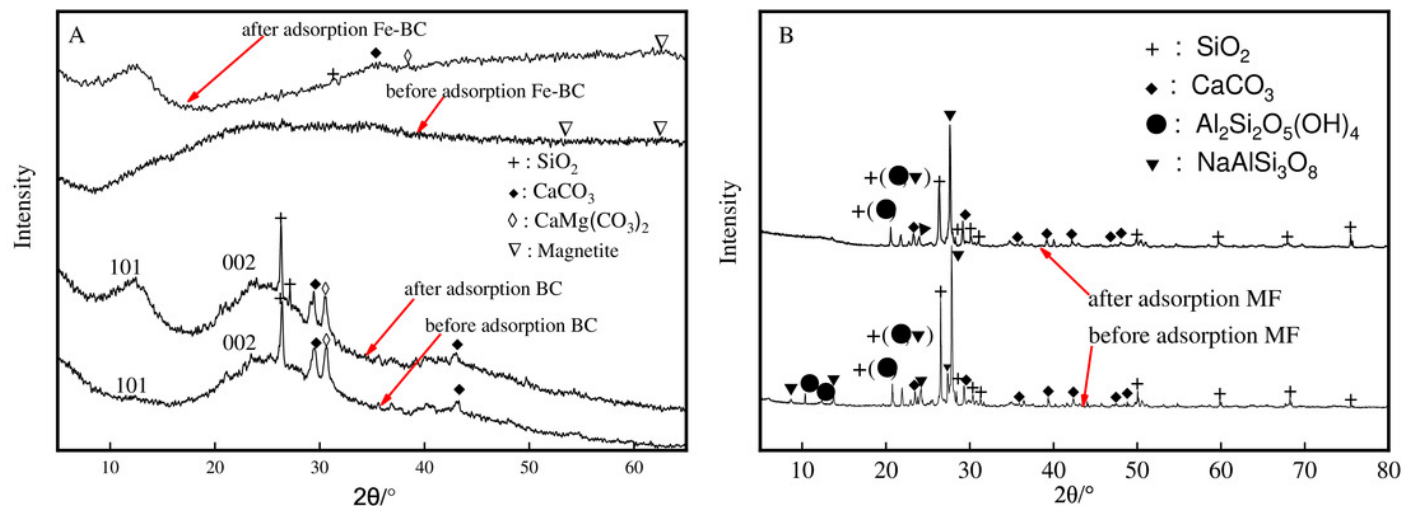
Figure 7

The heavy metal extraction fraction percentage in amendments after adsorption of Cu(A) and Cd(B).
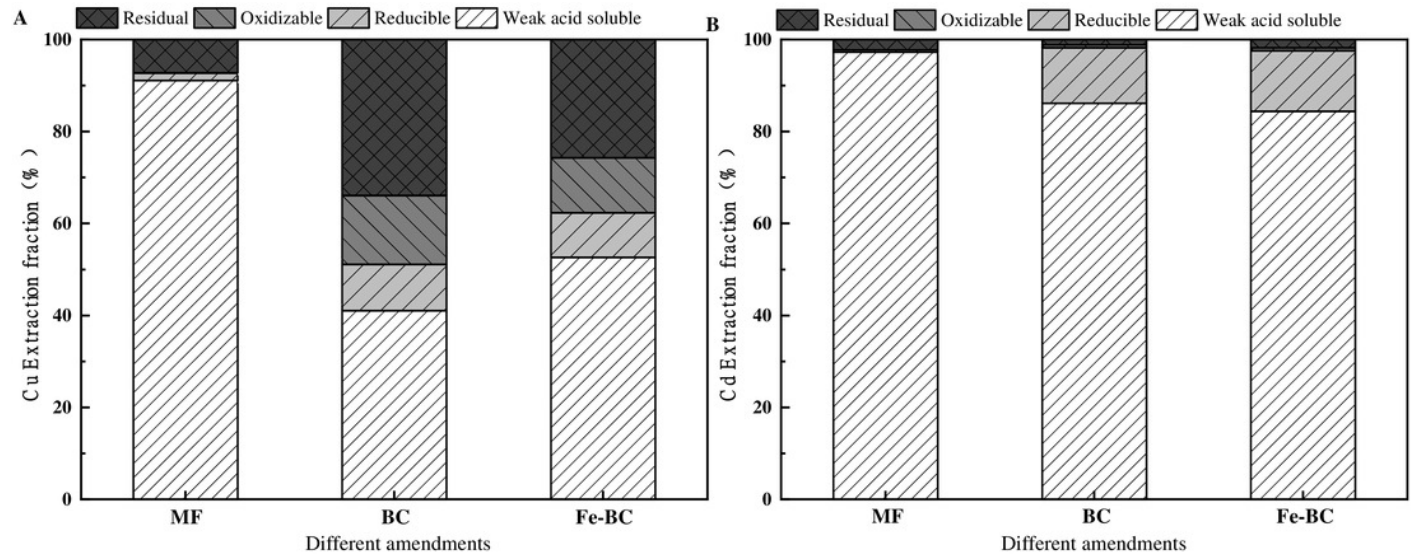
Figure 8

Effects of different amendments on the extract fraction of Cu(A) and Cd(B) in soil colloid